

1 | [December 15, 2020](#)

2  
3 **Temperature decadal trends, and their relation to diurnal variations in the lower**  
4 **thermosphere, stratosphere, and mesosphere, based on measurements from SABER on**  
5 **TIMED.**

6  
7 **Frank T. Huang<sup>1\*</sup>, Hans G. Mayr<sup>2\*</sup>**

8 <sup>1</sup>University of Maryland, Baltimore County, MD 21250, USA

9 <sup>2</sup>NASA Goddard Space Flight Center, Greenbelt, MD 20771, USA

10 \*retired

11  
12 **Abstract.** We have derived the behavior of decadal temperature trends over the 24 hours of local  
13 time, based on zonal averages of SABER data, years 2012 to 2014, 20 to 100 km, within 48° of  
14 the equator. Similar results have not been available previously. We find that the temperature  
15 trends, based on zonal mean measurements at a fixed local time, can be different from those  
16 based on measurements made at a different fixed local time. The trends can vary significantly in  
17 local time, even from hour to hour. This agrees with some findings based on night-time lidar  
18 measurements. This knowledge is relevant because the large majority of temperature  
19 measurements, especially in the stratosphere, are made by instruments on sun-synchronous  
20 operational satellites which measure at only one or two fixed local times, for the duration of their  
21 missions. In these cases, the zonal mean trends derived from various satellite data are tied to the  
22 specific local times at which each instrument samples the data, and the trends are then also  
23 biased by the local time. Consequently, care is needed in comparing trends based on various  
24 measurements with each other, unless the data are all measured at the same local time. A similar  
25 caution is needed when comparing with models, since the zonal means from 3D models reflect  
26 averages over both longitude and the 24 hours of local time. Consideration is also needed in  
27 merging data from various sources to produce generic, continuous longer-term records. Diurnal  
28 variations of temperature themselves, in the form of thermal tides, are well known, and are due  
29 to absorption of solar radiation. We find that at least part of the reason that temperature trends  
30 are different for different local times is that the amplitudes and phases of the tides themselves  
31 follow trends over the same time span of the data. Much of past efforts have focused on the  
32 temperature values with local time when merging data from various sources, and on the effect of  
33 unintended satellite orbital drifts, which result in drifting local times at which the temperatures  
34 are measured. However, the effect of local time on trends has not been well researched. We also  
35 derive estimates of trends by simulating the drift of local time due to drifting orbits. Our  
36 comparisons with results found by others (AMSU, lidar) are favorable and informative. They  
37 may explain at least in part, the bridge between results based on daytime AMSU data and night  
38 time lidar measurements. However, these examples do not a pattern make, and more  
39 comparisons and study are needed.

40  
41 **1.0 Introduction**

42 The understanding of decadal temperature trends in the middle and upper atmosphere is  
43 interesting scientifically and important for practical reasons. Global temperature trends have  
44 been researched for decades based on a variety of satellite and ground-based measurements.  
45 However, relatively few studies have focused on the behavior of trends as a function of local  
46 time. Past efforts have focused more on the local time variations of temperature themselves in

47 comparing or merging various data sets, and on accounting for drifts in local time of  
48 measurements due to satellite orbital stability.

49 Diurnal variations of temperatures themselves, in the form of thermal tides, are well known,  
50 and are a result of absorption of solar radiation (see Brasseur and Solomon [2005] and references  
51 therein).

52 Understanding the behavior of trends with local time can be important because the large  
53 majority of global temperature measurements, especially in the stratosphere, are made by sun-  
54 synchronous satellites whose instruments measure temperature at only one or two fixed local  
55 times, for the duration of their missions. In these cases, the zonal mean trends derived from  
56 various satellite data are tied to, and biased by the specific local times at which each instrument  
57 samples the data.

58 Care is then needed in comparing results of trends derived from various measurements which  
59 sample data at different local times. It is also needed when merging data from various sources to  
60 produce generic, continuous, longer-term records. In addition, the zonal means of 3D models are  
61 averages of temperatures over both longitude and the 24 hours of local time, and comparisons  
62 with trends based on data taken at fixed local times, or a subset of local times, can be  
63 problematic (Austin et al., 2008).

64 In the following, based on data from the Sounding of the Atmosphere using Broadband  
65 Emission Radiometry (SABER) instrument on the Thermosphere-Ionosphere-Mesosphere-  
66 Energetics and Dynamics (TIMED) satellite, we derive the local-time dependence of decadal  
67 temperature trends over the 24 hours of local time, from 2002 to 2014, from the stratosphere into  
68 the lower thermosphere (20 to 100 km), within 48° of the equator.

69 Comparable results for temperature trends have not been available previously.

70 Our starting point here is based on results from our past studies, also based on SABER data.  
71 Previously, we had estimated diurnal variations of the temperature (thermal tides) for each day,  
72 expressed in the form of five Fourier series components (Huang et al., 2010a). We had also  
73 derived zonal means of temperature that are averages over both longitude and local time for a  
74 latitude circle (Huang et al., 2006, Huang et al., 2010a). These ‘synoptic’ zonal means are  
75 important because it can then be compared directly with 3D models. Details are given in Section  
76 2.

77 Using these past results, we here derive the behavior of decadal temperature trends as a  
78 function of local time.

79 We find that the temperature trends, based on zonal mean measurements at a fixed local time,  
80 can be different from those based on measurements made at a different fixed local time. These  
81 variations of trends can be significant in all regions of our study, and can vary significantly even  
82 from hour to hour.

83 Our results suggest that part of the reason that temperature trends are different for different  
84 local times is that the tidal amplitudes and phases of the tides also follow trends over the time  
85 span of the data.

86 In the following, we compare with results of trends by others. Because trends vary with the  
87 time span considered, comparisons should cover similar times, and the opportunities are limited.  
88 Although the comparisons support our results of local time variations in trends, more  
89 comparisons are needed.

90 Global stratospheric data are largely from the NOAA series of operational satellites and the  
91 Earth Observing System of satellites. These are generally in sun-synchronous orbits, so that data  
92 are sampled at only one or two local times, which are fixed for the duration of the missions. The

93 operational satellites are meant in part to monitor the atmosphere over the longer term, and have  
94 been making measurements since the 1970s. Over the years, they are replaced as needed, in order  
95 to maintain a continuous record of data. However, there have been issues of data continuity and  
96 compatibility among the different satellites, related to data sampling, instrument calibration, and  
97 operation. Also, over the years, the orbits of some satellites have drifted from their planned sun-  
98 synchronous state, so that the local times at which the measurements are made have also drifted  
99 over several hours or more.

100 There have been group and individual efforts to combine and merge the data from different  
101 sources to obtain uniform, consistent, decades-long data bases for temperature (and others). Parts  
102 of the issues are concerned with differences due to local times when merging data. For example,  
103 Mears and Wentz [2016] have considered the sensitivity of temperature trends to “diurnal cycle  
104 adjustment”, and improved the consistencies of the different data sets caused by orbital drifts in  
105 local time, based on cross information from other satellites, and on general circulation models.  
106 Keckut et al., [2015] have also shown that considering atmospheric tides to account for  
107 differences among measurements of successive operational polar orbiting satellites would  
108 improve matters. Funatsu et al., [2008] have studied the differences among night time lidar data  
109 and daytime sun-synchronous satellite data. Randel et al, [2016], McLandress (2015), Zou et  
110 al.,[2014, 2016], among others, have also considered the issue of merged data from various  
111 sources, with consideration for differences due to effects of local time

112 These merged long-term datasets have general advantages of providing for studies of trends  
113 and responses to solar activity. However, as noted earlier, if the various data sets do not  
114 represent uniform sampling in local time, the merged data could be tagged by the biases in local  
115 times.

## 116 **2.0 Previous results**

118 Because we make use of our previous results of temperature diurnal variations and trends, we  
119 briefly review for the convenience of the reader. Our previous results on temperature trends were  
120 based only on zonal means that are averages over both longitude and local time. See Huang et al.,  
121 [2014, 2010a].

122 The SABER instrument was launched in December 2001 on the TIMED satellite (Russell et al.,  
123 1999). The data used here is version 2.0, level2A. The values are interpolated to 4-degree  
124 latitude and 2.5 km altitude grids, and zonal averages are taken for analysis.

125 SABER temperature measurements have been analyzed with success by us and by others.  
126 Zhang et al. [2006] and Mukhtarov et al. [2009] have derived temperature diurnal tides using  
127 SABER data, and Nath and Sridharan [2014] have derived temperature trends using the same  
128 SABER data, but without accounting for diurnal variations. We have derived variations with  
129 periods from less than one day (diurnal variations) up to multiple years (semiannual oscillations  
130 (SAO), quasi-biennial oscillations (QBO)), and one decade or more (responses to the solar cycle).  
131 See Huang et al. [2010a, 2014, 2016a, b].

132 In a previous paper, Huang and Mayr [2019] had also analyzed the effects of local time on the  
133 response of temperature (and ozone) to the solar cycle (~ eleven years).

## 134 **2.1 Diurnal variations**

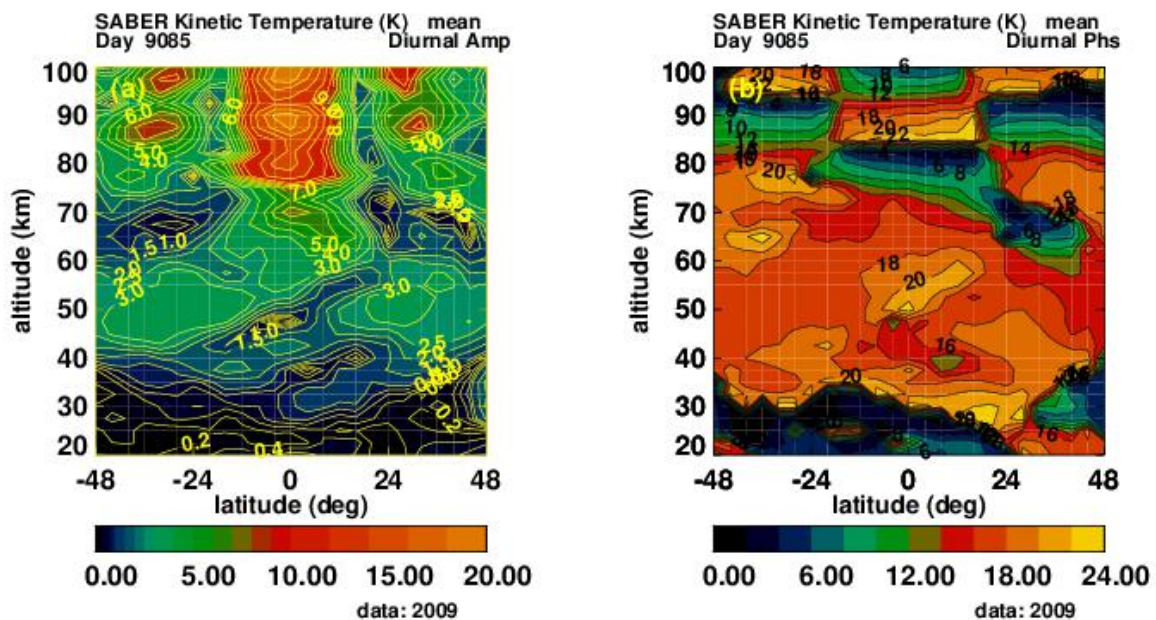
135 Due to the orbital characteristics of TIMED, SABER measurements provide the potential to  
136 estimate the variations of temperature as a function of the 24 hours of local time that data from  
137 other satellites generally do not provide. The local times of the SABER measurements decrease  
138

139 by about 12 min from day to day, and it takes 60 days to sample over the 24 hours of local time,  
140 using both ascending and descending node data. Although this provides essential information  
141 over the range of local times, over 60 days, variations can be due to both local time and other  
142 variables, such as season. Diurnal and mean variations are embedded together in the data and  
143 need to be unraveled from each other to obtain more accurate estimates of each.

144 Our algorithm is designed for this type of sampling in local time and provides estimates of  
145 both diurnal and mean (e.g., annual, semiannual, seasonal oscillations) variations together in a  
146 consistent manner. At a given latitude and altitude for zonal mean data over a period of a year,  
147 the algorithm performs a least squares estimate of a two-dimensional Fourier series, where the  
148 independent variables are local time and day-of-year, and variations as a function of local time  
149 and day-of-year are generated.

150 The fundamental Fourier period in day-of-year is 365 days, and that for local time is 24 hours.  
151 For subsequent months and years, the initial analysis serves as a sliding data window. To find  
152 subsequent monthly values, this window is advanced by one month, and the algorithm is applied  
153 again. Further details can be found in Huang et al.,[2010a].

154 Figure 1 shows an example of temperature diurnal amplitudes (left panel) and phases (right  
155 panel) of the diurnal tide on altitude-latitude coordinates (20 to 100 km, 48°S to 48°N), for day  
156 85 of 2009. Although not shown, higher components, such as the semidiurnal tides can also be  
157 significant. Our derivation includes 5 Fourier components.



158 **Figure 1.** Temperature tides from 20 to 100 km, 48°S to 48°N, day 85, year 2009. Left panel (a): diurnal amplitudes  
159 (K). Right (b): diurnal phases (hr maximum values).  
160  
161

## 162 2.2. Mean variations.

163 The zonal mean variations, which are averages over both longitude and local time, consistent  
164 with 3D models, are obtained together with the diurnal variations.  
165

166 Based on these zonal means, our earlier results of trends and decadal responses to solar activity  
167 had been presented in Huang et al. [2014, 2016a, 2016b, 2019].  
168

### 3.0 Current analysis

For the current analysis, we use the diurnal and mean variations together and generate zonal means at any selected local time.

In the following, we generate

- 1) Monthly zonal means that are averages over longitude, but at specific local times, to correspond to measurements by sun-synchronous satellites and night-time lidar measurements.
- 2) Monthly zonal means to simulate satellite orbital drifts, with local times that vary from month to month.
- 3) Monthly zonal means that are averages over longitude and the 24 hours of local time, as previously done.

From 1), 2), and 3) we estimate temperature trends using Equation (1), in a similar manner as previously done by others, and by us, using a multiple regression analysis that includes solar activity, trends, seasonal, quasi biennial oscillations (QBO), and local time terms, on monthly values. Specifically, the estimates are found from the equation

$$T(t) = a + b*t + c*S(t) + l*lst(t) + g*QBO(t) + d*F107(t) \quad (1)$$

where  $t$  is time (months),  $a$  is a constant,  $b$  is the trend,  $d$  the coefficient for solar activity (10.7 cm flux),  $c$  is the coefficient for the seasonal ( $S(t)$ ) variations,  $l$  the coefficient for local time ( $lst$ ) variations, and  $g$  the coefficient for the QBO. As is often done, the seasonal and local time variations are removed first, but we include them in Equation (1) for completeness. The F107 stands for the solar 10.7 cm flux, which is commonly used as a measure of solar activity, and the values used here are monthly means provided by NOAA.

$T$  stands for the various input temperature zonal means described in 1), 2), and 3), above.

The multiple regression is applied to the monthly zonal-mean values from June 2002 through June 2014 from 48°S to 48°N latitude, and from 20 to 100 km.

The analysis of uncertainties is the same for this study as for the previous study of the mean variations just described. Here the zonal means are generated at specific local times. Details and results of the statistical analysis are given in Huang et al., [2014, 2106a].

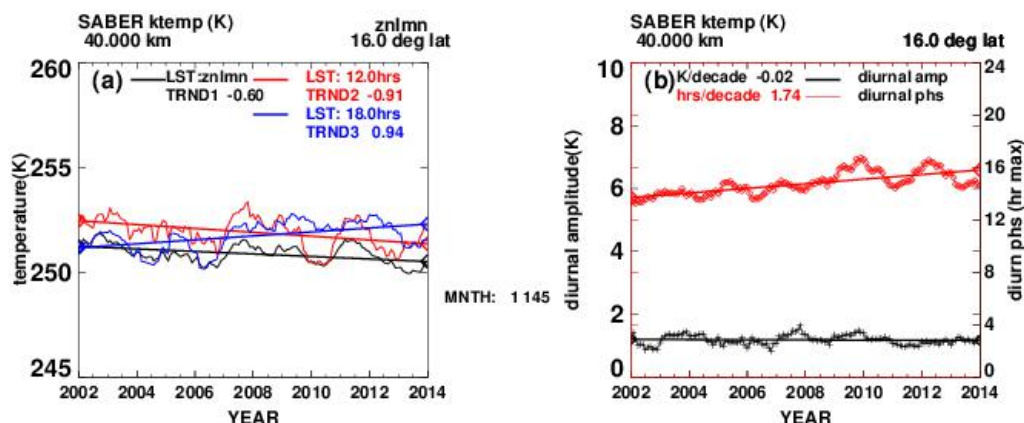
### 4.0 Current results: temperature trends as a function of local time

Before presenting our overall trend results as a function of local time, we first compare some specific results with those by others. The merged data sets noted earlier do not represent uniform averages over the range of local times nor do they represent specific fixed local times. In addition, they span a longer time interval than the SABER data, and we will not use them for comparisons. Because trends can significantly depend on the particular time period, comparisons are limited to the time span ~ 2002 to 2014.

Figure 2(a) (left panel) shows examples of our estimates of monthly SABER values of temperature (K) from mid 2002 to mid 2014, without the diurnal and seasonal variations. The black line shows zonal mean values that are averages over both longitude and local time at 40 km and 16° latitude, with a trend of ~ -0.6 K/decade, found from a linear fit. The red line shows monthly values of zonal means at a fixed 12 hrs local time, with a trend of ~ -0.91 K/decade. The blue line represents monthly values of zonal means at a fixed local time of 18 hrs, with a trend of ~ +0.94 K/decade. Figure 2(b) (right panel) shows the temperature tidal diurnal amplitude (black line, left hand scale) and the diurnal phase (red line, hour of maximum value, right hand scale).



215 The trends of the diurnal amplitudes and phases themselves contribute to the different  
 216 temperature trends at different local times. Although not shown, we note that semidiurnal tides  
 217 are not negligible. Additional plots corresponding to Figure 2(b) are given in the Appendix.  
 218



219 **Figure 2.** Left panel (a): Monthly SABER temperature (K) from 2002 to 2014, 40 km, 16°N latitude. Black line:  
 220 zonal mean values (averages over longitude and local time); red line: zonal mean at 12 hrs local time; blue line:  
 221 zonal mean at 18 hrs local time. Right panel (b): left axis scale: black line: tidal diurnal amplitude (K); red line, right  
 222 axis scale: diurnal phase (hr of maximum value).  
 223  
 224  
 225

#### 226 4.1 Stratosphere.

227 For the stratosphere, we compare with trends given by Funatsu et al.,[2016], based on data  
 228 from the Advanced Microwave Sounding Unit (AMSU) on the NASA Aqua satellite and from  
 229 night-time ground-based lidar measurements. The results of Funatsu et al.,[2016] are suitable for  
 230 comparison because the time span of the data are similar to ours (2002 to 2014), and AMSU  
 231 samples data near specific local times, namely, 13:30 and 1:30 local times.

232 Following Funatsu et al.,[2016], the AMSU is a cross-scanning microwave-based sounder and the  
 233 channels 9–14 sample with weighting functions peaking at approximately 18, 20, 25, 30, 35, and 40  
 234 km. The horizontal resolution at the near-nadir field of view is approximately 48 km, and the vertical  
 235 half width of the weighting functions is about 10 km.

236 Although the lidar measurements presented by Funatsu et al.,[2016] also cover a similar time  
 237 span (2002-2013), they are made only during night time from the Observatoire de Haute  
 238 Provence (OHP, 43.91°N, 5.71°E) and the Mauna Loa Observatory (MLO, 19.51°N, 155.61°W).

239 Figure 3 shows our results of temperature trends (K/decade) based on SABER data (2002 to  
 240 2014) and those from Funatsu et al.,[2016], based on AMSU and lidar measurements. For  
 241 AMSU, Funatsu et al., [2016] provide trends as a function of channel numbers for the low and mid  
 242 latitude composite trends, so following McLandress et al.,[ 2015], we use the altitudes of the  
 243 weighting function peaks, namely 20, 25, 30, 35, and 40 km, for comparison. They do provide  
 244 altitudes in km for comparison with lidar. We note that where the values and altitudes are given by  
 245 others such as Funatsu et al., [2016], we have transferred them manually to our figures, as needed.

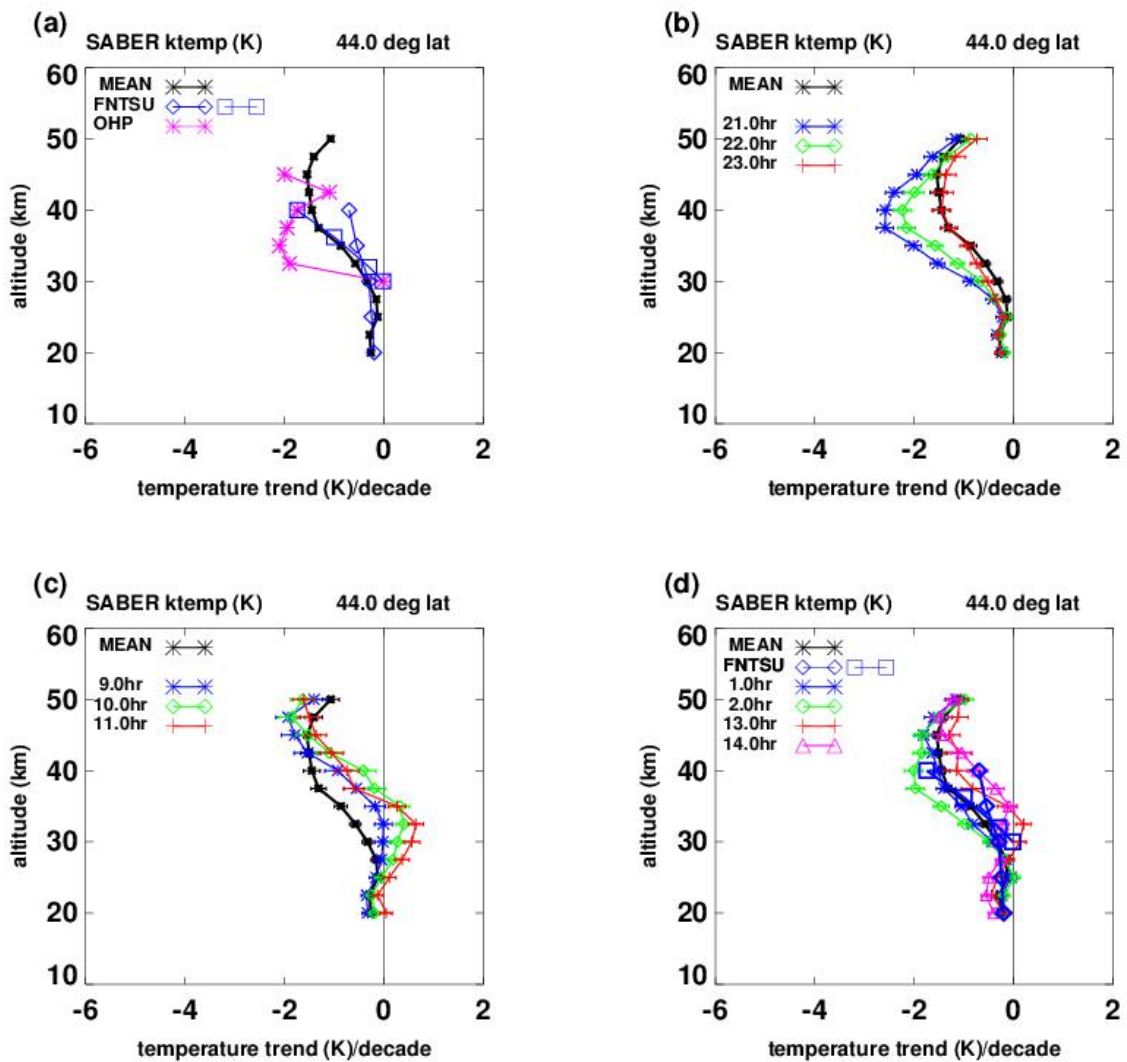
246 In the top left panel (a) of Figure 3, the black line plots trend results based on SABER zonal  
 247 means found by averages over both local time and longitude. The blue diamonds and squares are  
 248 from Funatsu et al.,[2016], based on AMSU data, presumably averages taken near 1:30 and  
 249 13:30 hours. The blue diamonds denote zonal mean trends for mid latitudes (30° to 60°N), and  
 250 the blue squares represent trends at 44°N to correspond to OHP. The blue squares are available

251 only from 30 to 40 km (~ 30, 32.0, 36.2, 40.0 km), but match our results (black line) at 44°N  
252 extremely well. The blue diamonds (from Funatsu AMSU, an amalgam to represent mid latitude)  
253 match our results almost exactly from 20 to 30 km, but are larger from 30 to 40km. This could  
254 simply be that the blue diamonds represent mid latitudes (30° to 60°N) while the blue squares  
255 and our black line represents trends at 44°N specifically. The magenta asterisks, also provided by  
256 Funatsu et al.,[2016], based on night-time lidar measurements at 44°N, are significantly more  
257 negative from 30 to 40 km than our results and those of the Funatsu et al.,[2016] AMSU. The top  
258 right panel (b) of Figure 3 shows our night time results from SABER at 21, 22, 23 hrs. It can be  
259 seen that our night time results agree better with the night-time lidar trends (magenta asterisks) in  
260 the left panel Figure 3(a). We do not know the details of the night-time hours of the lidar data.  
261 The bottom row left panel (c) of Figure 3 shows our daytime trends at 9, 10, 11 hrs, and agree  
262 less well with the lidar trends.

263 The average of all our night and daytime trends gives the zonal mean average shown by the  
264 black line. The bottom right panel (d) compares our results at 1, 2, 13, and 14 hrs with the  
265 AMSU results. They are near the local times of the AMSU data (presumably 1:30 and 13:30 hrs).  
266 It can be seen that the averages over the 4 local times compare favorably with those of Funatsu et  
267 al., [2016], based on AMSU data. It is not clear if Funatsu et al.,[2016] differentiated night from  
268 day measurements.

269 We believe that, by taking into account trends with local time, our results compare favorably  
270 with both the Funatsu et al., [2016] AMSU trends and their results based on night time lidar data.

271  
272



273  
 274 **Figure 3.** Temperature trends (K/decade, 2002-2014) vs altitude. Top left (a): Black asterisks: based on SABER  
 275 zonal means (over longitude and local time) at 44°N; blue diamonds: Funitsu Aqua trends for mid latitudes (30°-  
 276 60°N); blue squares: Funitsu Aqua trends at 44°N; magenta asterisks: based on night-time lidar measurements at  
 277 OHP (44°N). Top right (b): Black asterisks: same as (a), blue, green, red: our estimates at 21, 22, 23 hrs local time,  
 278 based on SABER data. Bottom left (c): Black asterisks: same as (a), blue, green, red: our estimates at 9, 10, 11 hrs  
 279 local time; bottom right (d): Black asterisks, same as (a); blue diamonds and squares: as in panel (a), Funitsu  
 280 AMSU, blue asterisks, green diamonds, red plusses, magenta triangles: SABER trends at 1, 2, 13, 14 hours.  
 281

282 The left panel of Figure 4 corresponds to that of Figure 3, but for 20°N to compare with  
 283 results of Funatsu et al., [2016] based on AMSU low-latitude and night-time lidar results at the  
 284 Hawaiian Mauna Loa Observatory (MLO, 19.51°N). As in Figure 3 for OHP, the lidar results  
 285 show a diversion to more negative trends near 30-35 km. Here, our results, as represented by  
 286 trends based on zonal means that are averages over local time also show a decrease, although not  
 287 as pronounced, near 30-35 km. As in Figure 3, both the blue diamonds and blue squares are from  
 288 Funatsu et al., [2016] based on AMSU data, but for low latitudes (0 to 30°N), and 20°N latitude,  
 289 respectively. They are smoother than our results between 25 and 40 km and do not show the



290 notch near 30 km that we and the lidar-based trends show. This could be due to the differences in  
 291 altitude resolution between AMSU and lidar and SABER data.

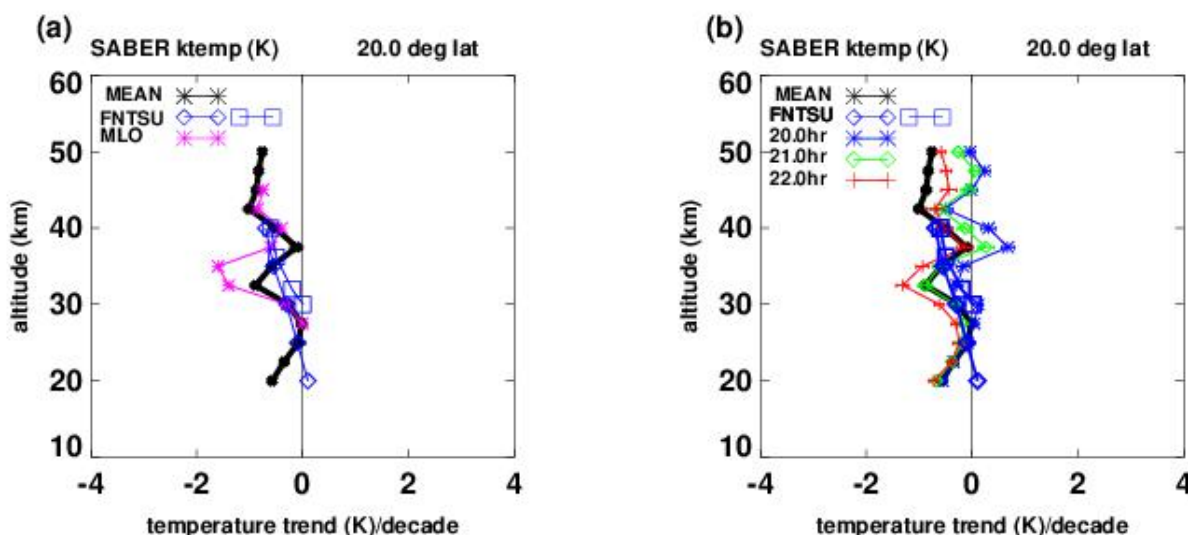
292 As can be seen in the right panel (b) of Figure 4, the decrease on our trends near 30 km is due  
 293 in large part to the behavior at 21 and 22 hours (green diamonds, red plusses).

294 Figures 3 and 4 show that by taking into account the different trends with local time, our  
 295 results compare more favorably with those of the Funatsu et al., [2016], based on AMSU and  
 296 lidar data. Figures 3 and 4 also show that trends can change significantly with local time, even  
 297 from hour to hour.

298 However, our comparisons do not a pattern make, and more comparisons are of course needed.

299 We note that the results of Khaykin et al.,[2017] based on analysis of GPS Radio Occultation  
 300 (GRO) measurements are in excellent agreement with AMSU (based on a slightly longer period  
 301 (2002-2016). Khaykin et al.,[2017] state that,” after down sampling of GRO profiles according  
 302 to the AMSU weighting functions, the spatially and seasonally resolved trends from the two data  
 303 sets are in almost exact agreement with trends based on AMSU data.”

304  
 305  
 306  
 307



308  
 309  
 310  
 311

312 **Figure 4.** Temperature trends (K/decade) vs altitude. Left (a): Black asterisks:trends based on SABER zonal  
 313 means (over longitude and local time) at 20°N; blue diamonds: Funitsu et al.,[2016] Aqua; data at 13.5 and 1.5 hrs,  
 314 low latitudes (0° to 30°N); blue squares: Funitsu Aqua at 20°N; magenta asterisks: lidar measurements at Mauna  
 315 Loa Observatory (MLO, 19.51°N), Right (b): Black asterisks: same as (a), blue, green, red: estimates at 20, 21,  
 316 22 hrs local time, based on SABER data.

317

### 318 4.2 Lower Thermosphere

319 In Figure 5, we compare our results (K/decade) with the lidar night-time measurements of She  
 320 et al.,[2019], at Fort Collins, CO. (41°N, 105°W)/Logan Utah (42°N, 112°W), from 2002-2014.

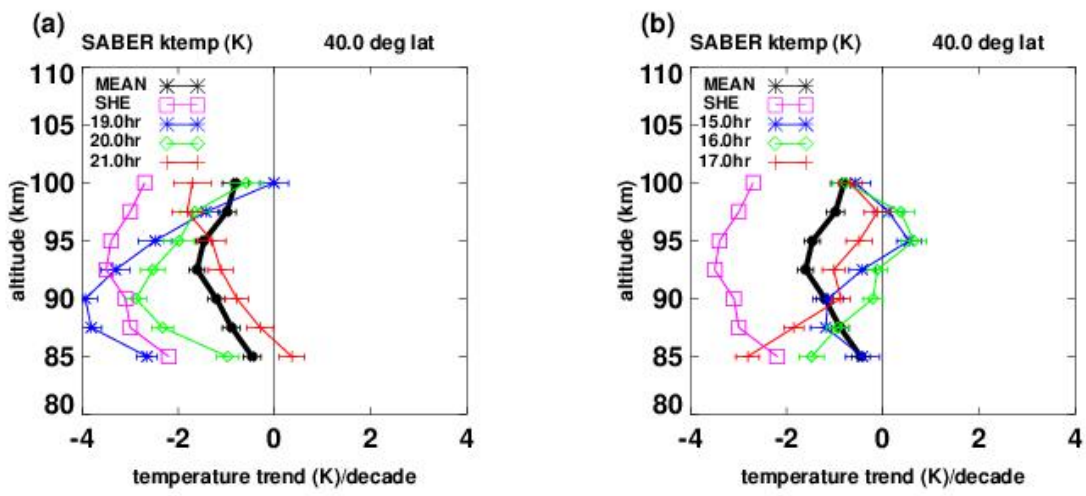
321 They actually made nocturnal temperature observations between 1990 and 2017, but divided  
 322 their analysis into various time periods, and smaller time intervals within the night time hours.

323 This provides valuable information regarding trends and local time. In the left panel (a) of Figure  
 324 5, the magenta squares denote the mean night time trends derived by She et al.,[2019]. The black  
 325 line represents our trend results based on zonal means (averages over longitude and local time),  
 326 while the blue asterisks, green diamonds, and red plusses show our zonal mean trends at 19, 20,  
 327 and 21 hours, respectively. In contrast, the right panel (b) of Figure 5 shows corresponding  
 328 results based on Saber data in the day time at 15, 16, 17 hours local time. We have not included  
 329 more local times due in part that the plots become busy, and some lines reach maximum and  
 330 minima at different altitudes. Overall, the averages of day time and night trends result in the  
 331 black line.

332 It can be seen in Figure 5 that, as in Figures 3 and 4, changes in trends over as little as an  
 333 hour of local time can be significant. These results show that there are systematic differences in  
 334 derived trends at different local times. This agrees with those of She et al., [2019], who have also  
 335 derived trends averaged over 2 hrs at midnight, and they are significantly different from those  
 336 found from the all-night mean measurements. She et al., [2019] provide midnight results only for  
 337 a much larger time span (March 1990 to December 2017), so we do not compare.

338 Considering that the lidar data are not zonal means, and the details of the night-time sampling  
 339 are probably different from ours, we believe that our results generally support those of She et al.,  
 340 [2019].

341



342

343

344 **Figure 5.** Temperature trends (K/decade) vs altitude, at 40°N latitude. Left (a): Black asterisks: trends based on  
 345 SABER zonal mean (over longitude and local time); blue asterisks, green diamonds, red plusses: trends based on  
 346 SABER zonal means at 19, 20, 21 hrs local time. Magenta squares: trends based on night-time lidar measurements  
 347 by She et al.,[2019]; Right (b): as in (a) but for SABER results at 15, 16, 17 hrs local time.

348

349

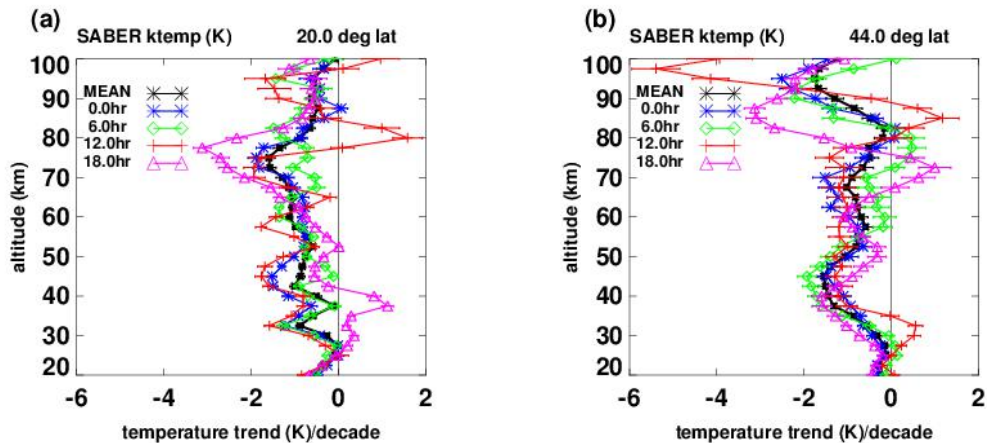
**4.3 General results and orbital drift.**

350 Figure 6 shows more generally our derived trends (K/decade) at 20°N (left panel) and 44°N  
 351 (right panel), from 20 to 100 km, at different local times. The blue asterisks, green diamonds, red  
 352 plusses, and magenta triangles represent 0, 6, 12, and 18 hrs, respectively. The salient features  
 353 are that the trends can vary significantly as a function of local time, even from hour to hour.

354 Because temperature trends can depend on the time period of the data or models, so may tidal  
 355 trends. So we should not assume that the local time behavior of trends for different time periods  
 356 will be necessarily consistent with each other.

357  
358  
359  
360  
361  
362

A broader and more detailed understanding would entail numerical studies, such as models which include studies of trends relating to local times. Then trends in thermal tides could be constrained to be zero to test effects on trends of the temperature.



363  
364  
365  
366  
367

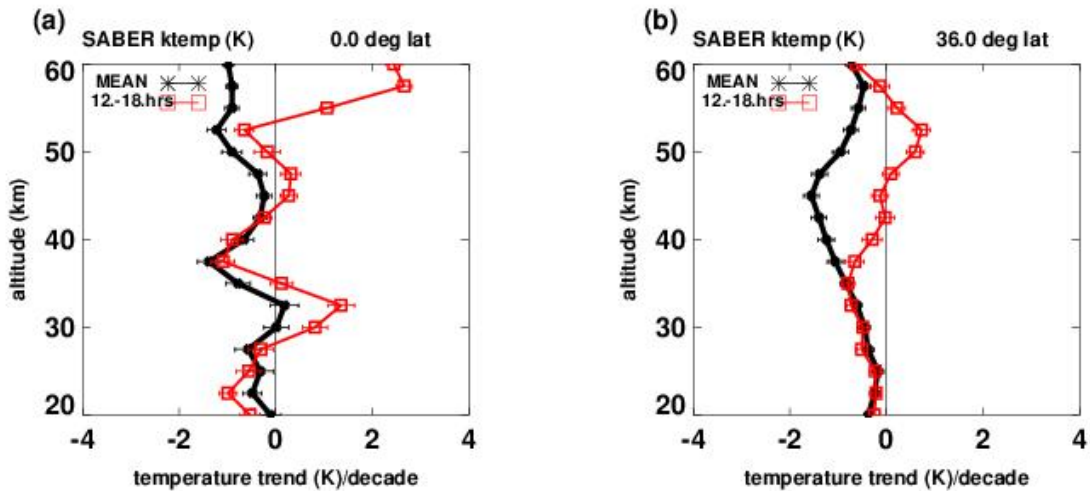
**Figure 6.** Temperature trends (K/decade) vs altitude from 20 to 100 km at 20°N (left panel) and 44°N (right panel). Black: trends based on SABER zonal means over longitude and local time; blue: based on zonal means at 0 hr; green: 6 hrs, red: 12hrs, magenta: 18 hrs local time.

368  
369  
370  
371  
372  
373

As noted earlier, over years, the orbits of some operational satellites have drifted from their intended sun-synchronous state, so that the local times at which measurements are made have also drifted, by several hours. As a simple simulated example, Figure 7 shows our results for temperature trends (K/decade) versus altitude, at the Equator (left panel) and at 36°N, from 20 to 60 km. The red squares denote trends where local times increased linearly from 12 to 18 hrs from 2002 to 2014, to simulate orbital drift. Black asterisks denote trends based on SABER data.

374  
375  
376  
377  
378  
379

To our knowledge, there have been no previous similar results on this subject, and Figure 7 is meant to provide only an indication of what may result when local times at which measurements are made are not controlled. Specifics would depend on the orbital drift of the particular satellite (Funatsu et al., 2016) and on the particular study.



380  
381  
382 **Figure 7.** Temperature trends (K/decade) vs altitude at the equator (left panel) and 36°N latitude (right panel).  
383 Black lines: trends based on SABER data (averaged over longitude and local time); red squares: estimated trends for  
384 cases where local times of measurements increase linearly from 12 to 18 hrs from 2002 to 2014.  
385

### 386 387 388 389 **5.0 Summary and conclusion**

390 Using SABER data, we have investigated the local time variations of temperature trends  
391 (K/decade) from 2002 to 2014, 20 to 100 km, and 48°S to 48°N latitude. SABER provides global  
392 temperature measurements over the 24 hrs of local time, and from 20 to 100 km in altitude, that  
393 are not available from other satellites and sources.

394 From our past studies based on SABER data, we had estimated diurnal variations of the  
395 temperature (thermal tides) for each day, expressed in the form of five Fourier series components  
396 (Huang et al., 2010a).

397 We had also derived zonal means of temperature that are averages over both longitude and  
398 local time for a latitude circle (Huang et al., 2006, 2010a). These ‘synoptic’ zonal means are  
399 important because they can then be compared directly with 3D models (Austin et. al., 2008).

400 As explained earlier, zonal means from sun-synchronous satellites are tied to one or two local  
401 times. To our knowledge, comparable zonal means of temperature that are averages over  
402 longitude and the 24 hours of local time are just not available elsewhere.

403 In this current study, we have combined the past results to estimate the zonal mean trends  
404 corresponding to specific local times.

405 These results at local times have not been available previously. They show that the values of  
406 temperature decadal trends for a fixed local time are different from trends at another fixed local  
407 time. We find that the amplitudes and phases of the tides themselves also display decadal trends  
408 and are then likely contributors to the local time variations of temperature trends.

409 Our results of trend variations with local time are supported by comparisons with  
410 corresponding nighttime lidar measurements in the stratosphere and lower thermosphere. They  
411 are also supported by comparisons with corresponding satellite measurements made at specific  
412 local times in the stratosphere.

413 The dependence of trends on local time is significant throughout the region of analysis, and can  
414 be significant even from hour to hour, as can be seen in Figures 3, 4, 5, and 6.

415 In the lower thermosphere, this agrees with [corresponding](#) trend results by She et al.,[2019],  
416 based on lidar night-time measurements. She et al., [2019] found that trends based on a two-hour  
417 average near midnight show systematic differences from the average over other hours. Our  
418 comparisons with the overnight results of She et al., [2019] are seen in Figure 5, where our  
419 trends at 19, 20, and 21 hours compare favorably, while our day time trends at 15, 16, and 17  
420 hours compare less favorably.

421 In the stratosphere, our comparison with trends found by Funatsu et al.,[2016], based on lidar  
422 and AMSU measurements, are even better, as seen in Figures 3 and 4. At 44°N (AMSU and  
423 OHP lidar), Funatsu et al., [2016] provide AMSU trend results only from 30 to 40 km, but they  
424 match our results almost exactly. Their results from 20 to 40 km, representing mid latitudes (30°  
425 to 60°N) also match our results almost exactly from 20 to 30 km, but are larger from 30 to 40km.  
426 Between ~ 30 to 40 km, the night-time lidar trends are significantly smaller (more negative) than  
427 both our and that of Funatsu et al.,[2016]. However, when the comparison is between night time  
428 lidar and our night-time results (21, 22, and 23 hours, see Figures 3a, 3b), the agreements are  
429 better. At 20°N (AMSU and MLO lidar), similar comments apply.

430 These examples all suggest that at least some of the differences between night time lidar  
431 trends and those based on other measurements that are not made at night, can be explained at  
432 least partly, through variations of trends with local time.

433 However, we emphasize that our three examples of course do not a pattern make, and more  
434 direct comparisons are needed. Our current comparisons are limited because the various results  
435 should be based on the similar time spans, and also not based on merged data from various  
436 sources, as the identity in local time would not be clear for merged data. Although there have  
437 been previous studies related to variations with local time, they focused on mitigating differences  
438 when merging data from different sources, and on accounting for temperature variations with  
439 local time due to orbital drifts.

440 Because our results show that the data sets representing measurements at different fixed local  
441 times can result in varying trends, merging those data can result in trends that cannot be tied to  
442 specific local times, or to averages over the 24 hours of local time, as in 3D models, and can  
443 result in biases.

## 444 Appendix

447 We present additional figures, corresponding to Figure 2(b), of temperature diurnal amplitudes  
448 and phases over more altitudes (20, 40, 60, 80, 90 km) and latitudes (0°, 40°).

449 The left panels (a) of each figure show temperature tidal diurnal amplitudes and phases at  
450 various altitudes and the Equator, while the right panels (b) correspond to the left panels but at  
451 40°N latitude. In each panel, the left axis scale and black line denote tidal diurnal amplitudes (K),  
452 while the right axis scale and red line show the diurnal phases (hr of maximum value).

453 The displayed trend values are obtained from a simple least squares straight line fit. The larger  
454 variations generally reflect modulation of the tides by the quasi biennial oscillation (QBO). This  
455 has been discussed in models (Mayr and Mengel, 2005) and other SABER data (Forbes et al.,  
456 2008).

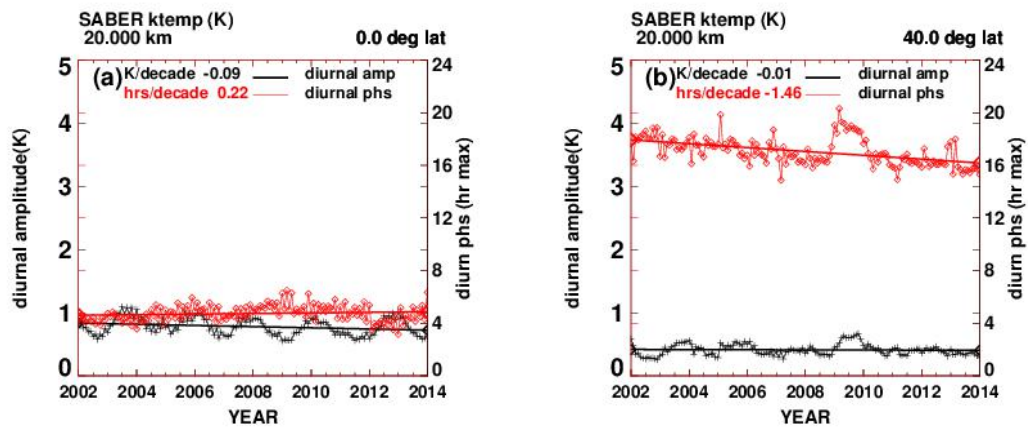
457 Although the figures may give additional insight to the nature of the trends, there are caveats to  
458 be considered. We note that the semidiurnal amplitudes and phases can also be significant. We



459 have derived a total of five Fourier components, and our numerical results reflect all 5 Fourier  
460 terms.

461 Because both amplitudes and phases exhibit trends, they need to be considered in parallel, in  
462 tandem, and this is difficult to discern, qualitatively. In addition, because the trends are generally  
463 small, it would be difficult to arrive at conclusions.

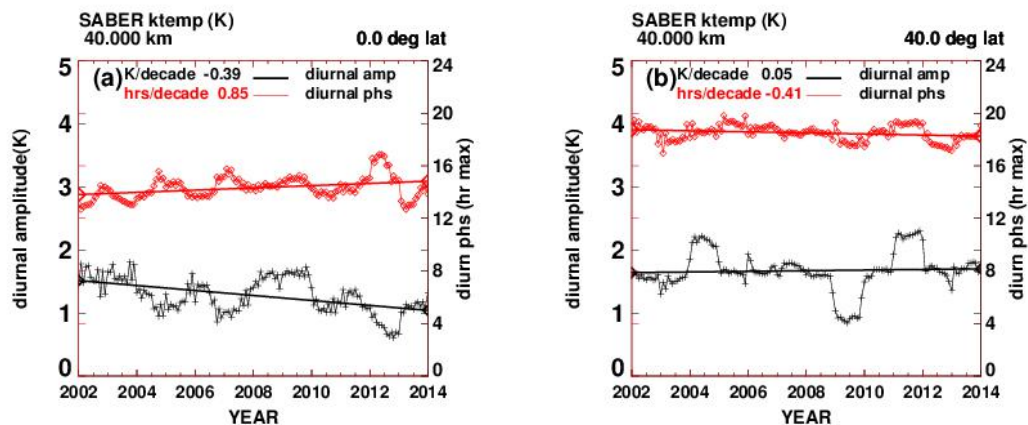
464



465 **Figure A1.** Left panel (a): Temperature tidal diurnal amplitudes and phases at 20 km and equator; left axis scale:  
466 black line: tidal diurnal amplitude (K); right axis scale: red line: diurnal phase (hr of maximum value). Right panel  
468 (b): as in left panel but at 40°N latitude.

469

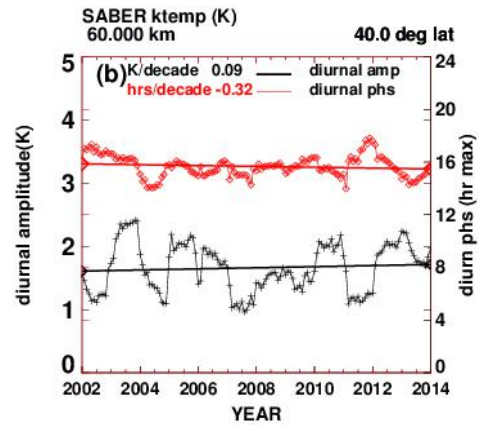
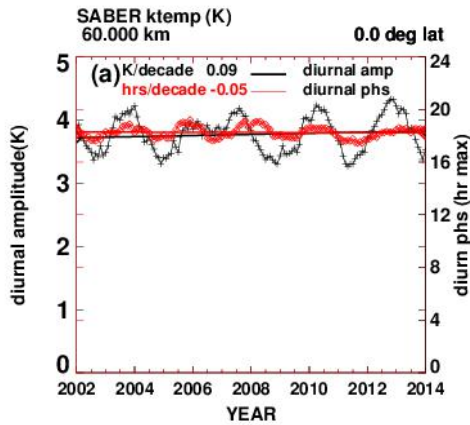
470



471 **Figure A2.** Left panel (a): Temperature tidal diurnal amplitudes and phases at 40 km and equator; left axis scale:  
472 black line: tidal diurnal amplitude (K); right axis scale: red line: diurnal phase (hr of maximum value). Right panel  
474 (b): as in left panel but at 40°N latitude.

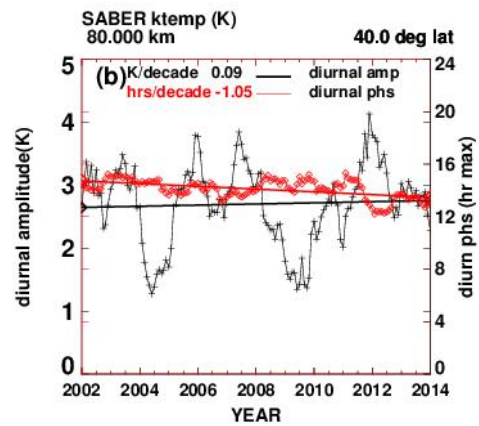
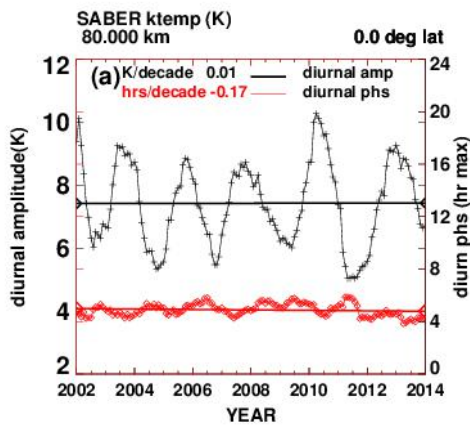
475





476  
477  
478  
479  
480  
481  
482

**Figure A3.** Left panel (a): Temperature tidal diurnal amplitudes and phases at 60 km and equator; left axis scale: black line: tidal diurnal amplitude (K); right axis scale: red line: diurnal phase (hr of maximum value). Right panel (b): as in left panel but at 40°N latitude.



483  
484  
485  
486  
487  
488

**Figure A4.** Left panel (a): Temperature tidal diurnal amplitudes and phases at 80 km and equator; left axis scale: black line: tidal diurnal amplitude (K); right axis scale: red line: diurnal phase (hr of maximum value). Right panel (b): as in left panel but at 40°N latitude.

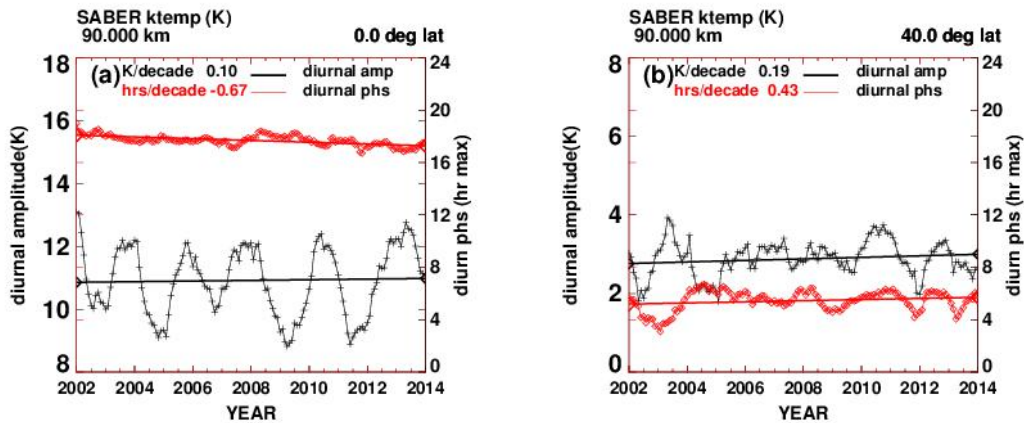


**Figure A5.** Left panel (a): Temperature tidal diurnal amplitudes and phases at 90 km and equator; left axis scale: black line: tidal diurnal amplitude (K); right axis scale: red line: diurnal phase (hr of maximum value). Right panel (b): as in left panel but at 40°N latitude.

489  
490  
491  
492  
493  
494  
495  
496

#### Data availability

The SABER data are freely available from the SABER project at <http://saber.gats-inc.com/>.

499

**Acknowledgements.** We thank the editor G. Stober and two anonymous referees, whose comments helped to improve the manuscript.

500  
501  
502  
503  
504

#### References

505  
506

Austin, J., Tourpali, K., Rozanov, E., Akiyoshi, H., Bekki, S., Bodeker, G., Brühl, C., Butchart, N., Chipperfield, M., Deushi, M., Fomichev, V. I., Giorgetta, M. A., Gray, L., Kodera, K., Lott, F., Manzini, E., Marsh, D., Matthes, K., Nagashima, T., Shibata, K., Stolarski, R. S., Struthers, H., and Tian, W.: Coupled chemistry climate model simulations of the solar cycle in ozone and temperature, *J. Geophys. Res.*, 113,D11306,<https://doi.org/10.1029/2007JD009391>, 2008.

511  
512  
513

Brasseur, G. P. and Solomon, S.: *Aeronomy of the Middle Atmosphere*, Springer, Dordrecht, The Netherlands, 2005.

514  
515  
516  
517

Forbes, J. M., Zhang, X., Palo, S., Russell, J, Mertens, C. J., and Mlyneczek, M.: Tidal variability in the ionospheric dynamo region, *J. Geophys. Res.*, 113, A02310, [doi:10.1029/2007JA012737](https://doi.org/10.1029/2007JA012737), 2008.

518  
519  
520

Funatsu, B.M., Claud, C., Keckhut, P., and Hauchecorne, A.: Cross-validation of Advanced Microwave Sounding Unit and lidar for long-term upper-stratospheric temperature monitoring, *J. Geophys Res*, 113, D23108, [doi:10.1029/2008JD010743](https://doi.org/10.1029/2008JD010743), 2008.

521  
522  
523

Funatsu, B. M., Claud, C., Keckhut, P., Hauchecorne, A., and Leblanc, T.: Regional and seasonal stratospheric temperature trends in the last decade (2002–2014) from AMSU observations, *Journal of Geophysical Research: Atmospheres*

524 | 10.1002/2015JD024305, [8172-8185](#), July, 2016.

525 | [Huang, F. T., Mayr, H. G., C. A. Reber, C. A., Russell, J. M., III, Mlynczak, M., Mengel, J.:](#)

526 | [Zonal-mean temperature variations inferred from SABER measurements on TIMED compared](#)

527 | [with UARS observations, J. Geophys Res, 111, A10S07, doi:10.1029/2005JA011427, 2006](#)

528 | Huang, F. T., McPeters, R. D., Bhartia, P. K., Mayr, H. G., Frith, S. M., Russell III, J. M., and

529 | Mlynczak, M. G.: Temperature diurnal variations (migrating tides) in the stratosphere and lower

530 | mesosphere based on measurements from SABER on TIMED, J. Geophys. Res., 115, D16121,

531 | doi:10.1029/2009JD013698, 2010a.

532 | [Huang, F. T., Mayr, H. G., Russell III, J. M., and Mlynczak, M. G.: Ozone and temperature](#)

533 | [decadal trends in the stratosphere, mesosphere and lower thermosphere, based on](#)

534 | [measurements from SABER on TIMED, Ann. Geophys., 32, 935–949,](#)

535 | <https://doi.org/10.5194/angeo-32-935-2014>, 2014.

536 | [Huang, F. T., Mayr, H. G., Russell III, J. M., and Mlynczak, M. G.: Ozone and temperature](#)

537 | [decadal responses to solar variability in the mesosphere and lower thermosphere, based on](#)

538 | [measurements from SABER on TIMED, Ann. Geophys., 34, 29–40,](#)

539 | <https://doi.org/10.5194/angeo-34-29-2016>, 2016a.

540 | [Huang, F. T., Mayr, H. G., Russell III, J. M., and Mlynczak, M. G.: Ozone and temperature](#)

541 | [decadal responses to solar variability in the stratosphere and lower mesosphere, based on](#)

542 | [measurements from SABER on TIMED, Ann. Geophys., 34, 801–813,](#)

543 | <https://doi.org/10.5194/angeo-34-801-2016>, 2016b.

544 | Huang, F. T., and Mayr, H. G.: Ozone and temperature decadal solar-cycle responses, and

545 | their relation to diurnal variations in the stratosphere, mesosphere, and lower thermosphere,

546 | based on measurements from SABER on TIMED, Ann. Geophys., 37, 471–485, 2019

547 | <https://doi.org/10.5194/angeo-37-471-2019>.

548 | Keckhut, P., Funatsu, B. M., Claud, C., and Hauchecorne, A.: Tidal effects on stratospheric

549 | temperature series derived from successive advanced microwave sounding units,

550 | Quarterly Journal of the Royal Meteorological Society, 141, 477–483, B, doi:10.1002/qj.2368,

551 | 2015

552 | Khaykin, S.M., Funatsu, B. M., Hauchecorne, A., Godin-Beekmann, S., Claud, C., Keckhut,

553 | P., Pazmino, A., Gleisner, H., Nielson, J. K., Syndergaard, S., and Lauritsen, K. B.:

554 | Postmillennium changes in stratospheric temperature consistently resolved by GPS radio

555 | occultation and AMSU observations Geophys. Res. Lett, 10.1002/2017GL074353, July, 2017.

556 | [Mayr, H.G., J. G. Mengel, Interannual variations of the diurnal tide in the mesosphere generated](#)

557 | [by the quasi-biennial oscillation, https://doi.org/10.1029/2004JD005055, 2005.](#)

558 | Mears, C. A., and Wentz, F. J.: Sensitivity of Satellite-Derived Tropospheric Temperature

559 | Trends to the Diurnal Cycle Adjustment. Journal of Climate, 29, 3629–3646,

560 | <http://dx.doi.org/10.1175/JCLI-D-15-0744.s1>, 2016.

561 | McLandress, C., Shepherd T. G., Jonsson, A. I., von Clarmann, T., and Funke, B.: A method

562 | for merging nadir-sounding climate records, with an application to the global-mean stratospheric

563 | temperature data sets from SSU and AMSU, Atmos. Chem. Phys., 15, 9271–9284, 2015,

564 | doi:10.5194/acp-15-9271-2015

565 | Mukhtarov, P., Pancheva, D., and Andonov, B.: Global structure and seasonal and interannual

566 | variability of the migrating diurnal tide seen in the SABER/TIMED temperatures between 20

567 | and 120 km, J. Geophys. Res., 114, A02309, doi:10.1029/2008JA013759, 2009

568 Nath, O., and Sridharan, S.: Long-term variabilities and tendencies in zonal mean TIMED–  
569 SABER ozone and temperature in the middle atmosphere at 10–15°N, *J. Atmos. Solar-Terr. Phys.*,  
570 120, 1–8, 2014.

571 Randel, W. J., Smith, A. K., Wu, F., Zou, C.-Z., and Qian, H.: Stratospheric temperature  
572 trends over 1979–2015 derived from combined SSU, MLS, and SABER satellite observations,  
573 *J. Climate*, 29, 4843–4859, <https://doi.org/10.1175/JCLI-D-15-0629.1>, 2016.

574 Russell, III J. M., Mlynczak, M. G., Gordley, L. L., Tansock, J., and Esplin, R.: An overview  
575 of the SABER experiment and preliminary calibration results, *Proceedings of the SPIE*, 44th  
576 Annual Meeting, Denver, Colorado, July 18-23, 3756, 277–288, 1999.

577 Zhang, X., Forbes, J. M., Hagan, M. E., Russell III, J. M., Palo, S. E., Mertens, C. J., and  
578 Mlynczak, M. G.: Monthly tidal temperatures 20–120 km from TIMED/SABER, *J. Geophys.*  
579 *Res.*, 111, A10S08, doi:10.1029/2005JA011504, 2006.

580 Zou, C.-Z., Qian, H., Wang, W., Wang, L., and Long, C.: Recalibration and merging of SSU  
581 observations for stratospheric temperature trend studies, *J. Geophys. Res.*, 119, 13180–13205,  
582 doi:10.1002/2014JD021603, 2014.

583 Zou, C.-Z., Qian, H., Stratospheric Temperature Climate Data Record from Merged SSU and  
584 AMSU-A Observations, *J. Atm. and Oceanic Tech.*, 2016, doi: 10.1175/JTECH-D-16-0018.1  
585